Aust. J. Chem. **xxx**
https://doi.org/xxx

Full Paper

Electrochemical Properties of a Verdazyl Radical in Room Temperature Ionic Liquids

Junqiao Lee[A] *Chiara Caporale*,[A] *Allan J. McKinley*,[B] *Rebecca O. Fuller*,[A,C] *and Debbie S. Silvester*[A,D]

[A] Curtin Institute for Functional Molecules and Interfaces, School of Molecular and Life Sciences, Curtin University, GPO Box U1987, Perth 6845, Western Australia, Australia

[B] Chemistry, School of Molecular Sciences, The University of Western Australia, 35 Stirling Highway, Crawley, Western Australia 6009, Australia

[C] Present address: School of Natural Sciences-Chemistry, University of Tasmania, Hobart, Tasmania 7001, Australia

[D] Corresponding author, email: d.silvester-dean@curtin.edu.au, phone: +61(0)892667148

(Invited contribution for the special issue *Women in Chemistry II*)

Abstract

Room temperature ionic liquids (RTILs) have been widely investigated as alternative electrochemical solvents for a range of dissolved species over the past two decades. However, the behaviour of neutral radicals dissolved in RTILs is relatively unexplored. In this work, the electrochemistry of a stable verdazyl radical – 1,5-dimethyl-3-phenyl-6-oxoverdazyl (MPV) – has been studied on a platinum thin-film electrode using cyclic voltammetry and chronoamperometry in ten different RTILs. The organic solvent propylene carbonate is also employed as a comparison. The nature of the solvent system was found to have a large effect on the electrochemical behavior, particularly on the reduction reaction of the verdazyl radical. Chronoamperometry on a microdisk electrode was used to calculate diffusion coefficients (*D*'s), and plots of *D* vs the inverse of viscosity were linear, suggesting typical hydrodynamic diffusional characteristics of the radical, in line with the behaviour of dissolved neutral and charged compounds (e.g. ferrocene and cobaltocenium) in RTILs. Overall, this study demonstrates that different RTILs have a significant influence on the electrochemistry of MPV, and therefore careful selection of the solvent system for electrochemical applications is advised.

Introduction

Room-temperature ionic liquids (RTILs) are a unique class of solvents that are made up entirely of cations and anions. They are increasingly being recognised as ideal alternative electrolytes in a multitude of traditional and emerging electrochemical applications, such as batteries, sensors, actuators, capacitors, fuel cells, and photovoltaics.[1-6] They can effectively be described as an 'electrolyte solvent' as they serve as both the solvent and electrolyte in electrochemical experiments. RTILs have many key advantages over conventional solvents, including intrinsic ionic conductivity, high thermal and chemical stability, low volatility, good solvating properties, and wide electrochemical windows.[7-10] To understand their viability for use in different electrochemical applications, the fundamental electrochemical behaviour of dissolved species in RTILs must first be understood. Many electrochemical studies have been performed in RTILs, and the voltammetry has been compared and contrasted to conventional solvents in an extensive review paper.[11]

One type of dissolved species that has received less attention in RTILs are neutral radical compounds. Evans et al.[12] studied the stable free radical 2,2,6,6-tetramethylpiperidine-*N*-oxyl (TEMPO) by cyclic voltammetry in five RTILs, observing differences in the voltammetry in two tetraalkylphosphonium ionic liquids. This was attributed to the formation of a more ordered bilayer structure consisting of alternating ionic and lipophilic regions. The mechanisms and reactions of some charged radical species – including the *N,N,N′,N′*-tetramethyl-para-phenylenediamine (TMPD) radical cation,[13] and the 1-bromo-4-nitrobenzene radical anion[14] – have been studied in RTILs. We note that many electrogenerated species in RTILs are radicals (e.g. superoxide radical anion,[15] *N*,*N*-dimethyl-*p*-toluidine (DMT) radical cation[16]) but their behaviour is often difficult to assess because of their short-lived nature at the electrode. In this work, the electrochemistry of a stable neutral verdazyl radical is studied in a range of RTILs to expand the knowledge of radical electrochemistry in these solvent systems.

Neutral radicals are molecules that contain one (or more) unpaired electrons. These species do not obey conventional bond valence theory and as a result have fewer bonds than predicted, leading to the molecules being highly reactive and short lived.[17] However, there are a number of stable organic radicals that exist.[18] Stability in these systems tends to arise from the resonance delocalisation of unpaired spin and in some cases the steric protection of the high spin electron density. A number of applications are being developed based on stable radicals due to their unique redox properties.[19] Examples include both the development of species for use as single component conductors[20-21] and organic batteries.[22-23] It is the electron-transfer chemistry of these molecules which determines the usefulness of radical species, such as redox potentials.[24-25] Electrochemistry is an essential tool used to understand these processes.[26-27]

Verdazyls (Type I and II) are one such highly stable organic radical system (Fig. 1).[28-30] These heterocyclic molecules have an unpaired spin density that is delocalised over the nitrogen atoms. These molecules are stable in both air and water making them ideal candidates for understanding the electrochemical properties associated with the unpaired electrons. Type II verdazyls have been shown to be difficult to oxidize due to the electron withdrawing nature of the carbonyl functionality.[24, 31] The twisting of the molecule around the N-substituents can further add to this as it is associated with a decrease in the delocalisation of the unpaired electron.[32] Based on our literature search, the electrochemistry of various verdazyl (Type I and II) molecules has been studied

previously in various conventional solvents and mixtures (e.g. THF, triethylamine, acetonitrile, etc.),[24-25] but not in RTILs. In conventional solvents, the verdazyls were observed to undergo a one-electron oxidation from the neutral 7π radical to the 6π cation, and a one-electron reduction to the 8π anion (Fig. 2).[24] The oxidation and reduction potentials are significantly affected by the electron donating and withdrawing substituents present on the radical.[24] The 1,5-dimethyl-3-phenyl-6-oxoverdazyl (MPV) molecule, with methyl as both the R_1 and R_2 substituents, will be the focus of this work (Fig. 3). This radical has specifically been explored as a mediator in RAFT polymerization of styrene and *n*-butyl acrylate.[33-34]

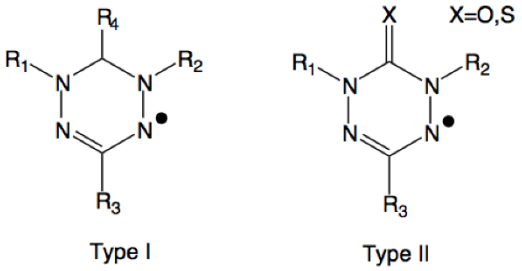

Fig. 1 Type I and II verdazyl radicals

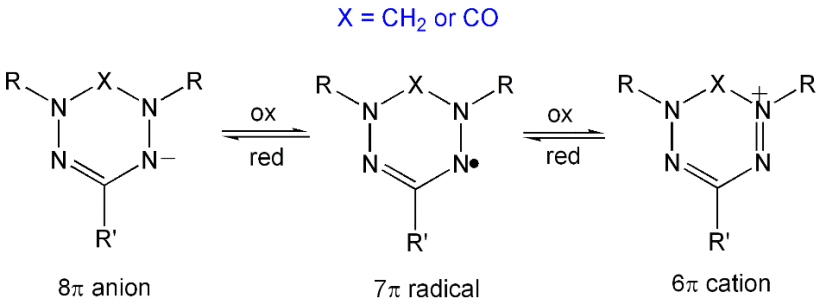

Fig. 2 Proposed mechanism for verdazyl radicals in conventional organic solvents adapted from Gilroy et al.[24]

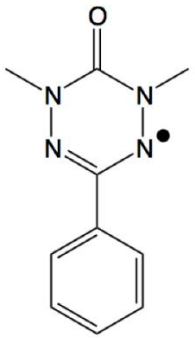

Fig. 3 Chemical structure of the Type II verdazyl, 1,5-dimethyl-3-phenyl-6-oxoverdazyl (MVP) used in this work.

Given the obvious advantages of RTILs as solvent systems, and the potential applications of the family of verdazyl radicals, we present a first look into the electrochemical mechanism of MPV (Fig. 3) in RTILs. We discuss the relationship between diffusion coefficient and solvent viscosity in terms of hydrodynamic theory and Stokes-Einstein behaviour. The findings in this study will be valuable in the understanding of the effect of solvation on the electrochemical behavior of a neutral radical, and to guide the selection of solvents for different electrochemical applications of these emerging and interesting materials. Additionally, understanding the electrochemistry of verdazyl radicals in RTILs is of great significance in future applications where they may be used concomitantly. An example is in batteries, where improved energy density can be achieved by increasing the concentration of the redox species in the catholyte. The use of RTILs with a stable and soluble redox compound is one solution for the development of new battery materials with higher energy storage

capabilities.[35] The stable verdazyl radical is a good candidate for such applications and warrants greater investigation to understand the underlying electrochemical behaviour of this species in RTILs.

Experimental

Chemicals and reagents

All reagents for the synthesis of MPV (see Supporting Information) were purchased from Sigma-Aldrich or Alfa Aesar and used without further purification, unless otherwise stated. The RTILs 1-ethyl-3-methylimidazolium bis(trifluoromethylsulfonyl)imide ($[C_2mim][NTf_2]$), 1-butyl-3-methyl-imidazolium bis(trifluoromethylsulfonyl)imide ($[C_4mim][NTf_2]$), *N*-butyl-*N*-methylpyrrolidinium bis(trifluoro-methylsulfonyl)imide ($[C_4mpyrr][NTf_2]$), and 1-butyl-3-methylimidazolium tetrafluoroborate ($[C_4mim][BF_4]$) were obtained from IoLiTec (Heilbronn, Germany) at the highest purity available (> 99.5 %). The RTILs 1-hexyl-3-methylimidazolium trifluorotris(pentafluoroethyl)phosphate ($[C_6mim][FAP]$), 1-butyl-3-methyl-imidazolium hexafluorophosphate ($[C_4mim][PF_6]$), and trihexyltetradecylphosphonium pentafluoroethyl-trifluorophosphate ($[P_{14,6,6,6}][FAP]$) were purchased from Merck KGaA (Kilsyth, Victoria, Australia) at "ultra-high" purity (< 99 %) grade. The RTIL trihexyltetradecyl-phosphonium bis(trifluoromethylsulfonyl)imide ($[P_{14,6,6,6}][NTf_2]$), kindly donated by Prof Chris Hardacre, and was synthesized according to standard literature procedures.[36-37] The chemical structures and abbreviations of RTIL cations and anions are shown in the Supporting Information. All RTILs were used as received, however, the blank voltammetry of all RTILs were tested to ensure that there were no obvious voltammetric features from impurities within the available potential window relative to the measured peaks. Propylene carbonate (PC, anhydrous, 99.7 %), ferrocene (Fc, $Fe(C_5H_5)_2$, 98 %) and tetra-*N*-butylammonium perchlorate (TBAP, 98 %), acetonitrile (MeCN, 99.8 %), methanol (99.9 %), and acetone (99.9 %) purchased from Sigma-Aldrich (NSW, Australia), and ultrapure water (resistance = 18.2 MΩ·cm, prepared by an ultrapure laboratory water purification system from Millipore Pty Ltd., North Ryde, NSW, Australia) were used for rinsing the electrodes before and after use. Hexaammineruthenium(III) chloride Ru(III)Hex, 98% (Sigma-Aldrich) and potassium chloride (KCl, > 99.5%, Fluka, Buchs, Switzerland) were used to prepare a 1 mM solution of Ru(III)Hex with 0.1 M $KCl_{(aq)}$ in ultrapure water for the calibration of the microdisk electrode radius.

Synthesis and characterisation of verdazyl radical

Detailed synthetic procedures for the verdazyl radical used in this work are reported in the Supporting Information. All reactions were carried out using aerobic conditions with magnetic stirring, unless otherwise stated. All reaction temperatures refer to oil bath temperatures. Thin layer chromatography (TLC) was performed on Merck silica gel 60 F_{254} pre-coated aluminium sheets. Visualisation of developed plates was achieved through the use of a 254 nm UV lamp. Column chromatography was performed using silica gel as supplied by Davisil® (chromatographic silica particle size: 40-63 µm).

Nuclear magnetic resonance spectra were recorded using a Bruker Advance 400 spectrometer (400 MHz for ^{1}H NMR; 100 MHz for ^{13}C NMR) at 300 K. All NMR spectra were calibrated to residual solvent signals. Data are reported as follows: chemical shift, multiplicity (app = apparent, s = singlet, d = doublet, t = triplet, q = quartet, m = multiplet, br = broad, sept = septet), integration, assignment and coupling constant. Infrared spectra

were recorded using an attenuated total reflectance PerkinElmer UATR Two Spectrum2 with a diamond stage. IR spectra were recorded from 4000-400 cm^{-1}. Melting points were determined using a BI Barnstead Electrothermal 9100 apparatus. UV absorption spectra were recorded on a Agilent Technologies Cary Series UV-vis Spectrophotometer in methanol using a cuvette with a 1.0 cm path length. Elemental analyses were carried out on bulk samples using a Thermo Finning EA 1112 Series Flash. ESR spectra of the resultant molecule were then recorded on a Bruker ESP300E spectrometer at room temperature (294 ± 1 K) with an ER4102ST cavity with the microwave frequency measured by the integral counter and the magnetic field measured by an ER035 NMR guassameter.

Instrumental

Electrochemical experiments were conducted using a PGSTAT101 Autolab potentiostat (Eco Chemie, Netherlands), interfaced to a PC with NOVA 1.11.2 software. The electrochemical cell was placed inside a custom-made aluminum Faraday cage in a fume cupboard at standard laboratory temperature (294 ± 1 K). For cyclic voltammetry (CV) experiments, platinum thin-film electrodes (TFEs, Micrux Technologies, Oviedo, Spain) were used, consisting of a 1 mm diameter Pt working electrode, together with Pt counter and reference electrodes in a planar configuration. Before employing the TFEs for mechanistic studies, they were first activated in a solution of 0.5 M H_2SO_4 by continuous CV cycling (ca. 50 cycles at 500 mV s^{-1}) over a potential range of -0.4 to 1.3 V. It was noted that the Pt electrode tends to foul after scanning the reduction peak of MVP, leading to an altered CV response. This was especially significant at low scan rates (e.g. 50 and 10 mV s^{-1}), and in the more viscous RTILs. Typically, the response recovers from fouling by waiting ~15 mins, so 15 mins was left between each CV scan to allow the system to fully recover.

The verdazyl radical was prepared in RTILs at a concentration of 10 mM and appeared to fully dissolve with no visible precipitates. A 15 μL aliquot of the radical solution in RTIL was then added onto the activated Pt-TFE for the voltammetry experiments. For experiments with ferrocene as an internal reference, a 15 μL aliquot of 2 mM Fc in MeCN was added onto the Pt-TFE at the end of each experiment and the MeCN was allowed to evaporate under a stream of nitrogen gas to leave a concentration of 2 mM in the RTIL/verdazyl solution.

For characterising the diffusion coefficient (*D*), a conventional two-electrode arrangement was employed, with a homemade platinum microelectrode (radius 8.29 ± 0.03 μm) as the working electrode and a 0.5 mm diameter silver wire (Sigma-Aldrich) as a combined counter electrode and quasi-reference electrode. The microdisk electrode was polished on soft lapping pads (Buehler, Lake Bluff, IL) with alumina powder of decreasing size (3, 1, and 0.5 μm, Kemet, NSW, Australia). The working electrode radius was calibrated using chronoamperometry with a 1 mM Ru(III)Hex in 0.1 $KCl_{(aq)}$ solution and adopting a value for the diffusion coefficient of 8.43×10^{-10} m^2 s^{-1} at 298 K.[38] A reservoir at the tip of the electrode was created with a segment of a 2–200 μL micropipette tip, into which microliter quantities (ca. 20 μL) of the RTIL could be placed. The electrodes were housed inside a glass 'T-cell',[39] and the RTIL containing the sample to be analysed was first purged under high vacuum (Edwards high vacuum pump, Model ES 50) to remove oxygen and dissolved atmospheric moisture for > 60 mins, before introducing N_2-gas at 1000 standard cubic centimetres per minute (sccm) under continuous flow during measurements.

Calculation of diffusion coefficients

Chronoamperometric transients were taken by holding the potential at 0 V for 60 s for pretreatment, before stepping to a potential after the first oxidation peak and holding for 10 s with a sampling rate of 0.01 s. Experimental data was modelled with the Shoup and Szabo approximation[40] using the nonlinear curve fitting function in Origin 8.6 (Herne Scientific Software, Australia). The equations used in the modelling of the chronoamperometric transients are:[40]

$$I = -4n\mathrm{FD}cr_d f(\tau) \quad (1)$$

$$f(\tau) = 0.7854 + 0.8863\tau^{-1/2} + 0.2146e^{-0.7823\tau^{-1/2}} \quad (2)$$

τ is the time constant given as follows,

$$\tau = \frac{4Dt}{r_d^3} \quad (3)$$

where n is the number of electrons transferred, F the Faraday constant, D the diffusion coefficient, c the initial concentration of the Type II verdazyl radical, r_d the microdisk electrode radius, and t the time. Experimental data was iteratively fitted using a fixed r_d (obtained from calibration), to obtain values of D in each RTIL.

Results and Discussion

Cyclic voltammetry of 1,5-dimethyl-3-phenyl-6-oxoverdazyl (MVP) in different solvents

The electrochemical behaviour of MPV in ten different RTILs was first investigated using cyclic voltammetry (CV) and compared with the behaviour in a conventional aprotic solvent, propylene carbonate (PC) with 0.1 M TBAP (Fig. 4). PC was selected due to its very low volatility (boiling temperature = 240 °C) and its properties as a 'versatile solvent for electrochemistry'.[41] For example, it has been used as a solvent for various applications including ammonia gas sensing.[42] The voltammetry of this particular verdazyl radical (Fig. 3) has not yet been reported in the literature, so its behaviour in a conventional solvent system such as PC is important to study.

The potentials are scanned positively over the oxidation peak, before reversing to scan over the reduction peak. The CVs in Fig. 4 were taken at a relatively fast scan rate of 2000 mV s^{-1}, since the electrode was observed to 'foul' during cathodic CV measurements, particularly at lower scan rates in some RTILs. The fouling is likely to be caused by the build-up of electrogenerated products from the reduction process – see discussion on the mechanism below. Due to the use of a quasi-reference electrode, the potentials of all CVs were corrected with respect to an internal reference – the ferrocene/ferrocenium (Fc/Fc^+) redox couple – to allow comparison of the redox potentials in the different solvents. The same reference system was used in the study of verdazyl radicals in acetonitrile and dichloromethane.[24-25]

As can be seen in Fig. 4, the CVs typically show one oxidation peak and one reduction peak, consistent with the general mechanism reported for verdazyl radicals in acetonitrile and dichloromethane (Fig. 2).[24] Additional oxidation and reduction peaks are observed when the scan range is increased (see supporting information Fig. S1), but the discussion will be limited to the first oxidation and first reduction peak only. The oxidation peak in Fig. 4 displays good chemical reversibility in all solvents – with the exception of $[C_4mim][BF_4]$ – as evidenced by the presence of an obvious reduction peak on the reverse scan. In $[C_4mim][BF_4]$, the 6π verdazyl cation likely reacts with the $[BF_4]^-$ anion, resulting in a loss of the reverse peak. A pre-peak shoulder is also observed in this RTIL, hinting of a different mechanism compared to the other RTILs.

The verdazyl radical reduction peak, however, exhibits vastly different voltammetry in the different solvents. In the conventional solvent, PC, the reduction is chemically reversible (Fig. 4a), although the CV shape is much broader compared to the oxidation peak, suggesting that the reduction step has more sluggish electrochemical kinetics (see discussion below). In most of the RTILs, the oxidative back-peak following the reduction process (oxidation of the 8π verdazyl anion back to the neutral radical) is absent, suggesting that the 8π verdazyl anion in unstable and probably reacts with the RTIL cation. The imidazolium cation is known to undergo proton abstraction from the C(2) position, in the presence of a strong base.[43] However, even in the sulfonium $[S_{2,2,1}]^+$, ammonium $[N_{4,1,1,1}]^+$ and pyrrolidinium $[C_4mpyrr]^+$ RTILs, the voltammetry shows similar behaviour (Fig. 4). The reduction peak in some RTILs shows a split-wave feature, further hinting of a more complicated mechanism at play. The only RTIL that displays a clear reverse peak is $[C_4mim][PF_6]$, but the current for the reduction peak is much larger than the oxidation peak, decreasing the likelihood that the reduction is a one-electron reversible reduction as described in Fig. 2. An obvious reduction peak is not observed in the RTILs $[P_{14,6,6,6}][NTf_2]$ and $[P_{14,6,6,6}][FAP]$, but the sloping current increase suggests that a reduction process is taking place. Unusual voltammetry of species dissolved in RTILs with the $[P_{14,6,6,6}]^+$ cation has been reported in the literature several times.[44-46] We note that water may also play a role in the mechanism, since water is known to be present at ppm

levels in RTILs even after rigorous drying procedures (e.g. under vacuum).[47] Our experiments were carried out under a constant stream of dry nitrogen at a high flow rate of 1000 sccm to ensure that the water content was kept as low as possible during the measurements, and that this effect is minimal.

Table 1 summarises the data extracted from the CVs in Fig. 4, including the peak potentials (E_p vs. Fc/Fc^+), peak currents (I_p) and the peak-to-peak separations (ΔE_p) of the oxidation and reduction peaks. For easy visualization of the differences between the solvents, histogram plots of these values are also provided in the supporting information (Fig. S2 and Fig. S3).

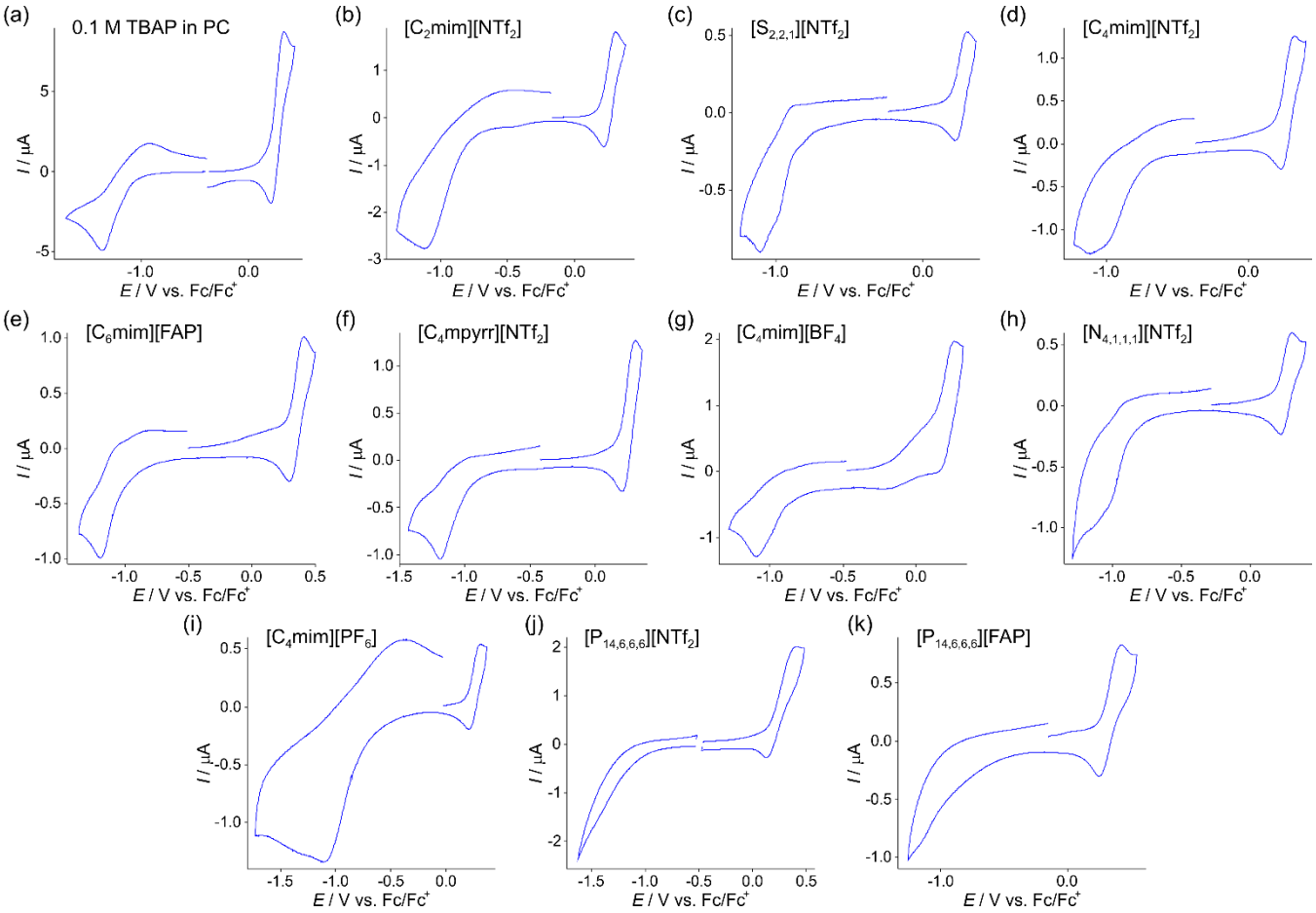

Fig. 4 Cyclic voltammograms of 10 mM MPV at a scan rate of 2000 mV s^{-1} on a Pt-TFE in: (a) PC (+0.1 M TBAP), (b) $[C_2mim][NTf_2]$, (c) $[S_{2,2,1}][NTf_2]$, (d) $[C_4mim][NTf_2]$, (e) $[C_6mim][FAP]$, (f) $[C_4mpyrr][NTf_2]$, (g) $[C_4mim][BF_4]$, (h) $[N_{4,1,1,1}][NTf_2]$, (i) $[C_4mim][PF_6]$, (j) $[P_{14,6,6,6}][NTf_2]$ and (k) $[P_{14,6,6,6}][FAP]$. The potentials were shifted so that the midpoint of the ferrocene/ferrocenium (Fc/Fc^+) redox couple was at 0 V.

The oxidation potentials (E_p) of the radicals were similar to that in PC at ca. 0.3 V vs. Fc/Fc^+ (Table 1), with the exception of $[C_6mim][FAP]$ and the two $[P_{14,6,6,6}]^+$ RTILs. The larger $[P_{14,6,6,6}]^+$ and $[FAP]^-$ ions probably provide poorer solvation of the electrogenerated verdazyl cation compared to the other RTIL ions, making the oxidation reaction less favourable. The reduction peak potential is more variable across the RTILs, ranging from -1.09 to -1.36 V, suggesting that the reduction mechanism is more strongly affected by the solvent environment compared to the oxidation reaction. Reduction potentials in the two $[P_{14,6,6,6}]^+$ RTILs could not be extracted from the CVs due to the absence of a clear peak. The 8π verdazyl anion therefore appears to be much less stable in RTIL environments compared to the 6π verdazyl cation.

Table 1 Peak potentials, E_p, peak currents, I_p, and peak-to-peak separations, ΔE_p, for the CV of 10 mM MPV at 2000 mV s^{-1}. Data extracted from CVs in Fig. 4 and Fig. S1. Numbers in brackets are estimated because of the absence of a clear peak

	Oxidation			Reduction		
Electrolyte	E_p / mV vs. Fc/Fc^+	I_p / µA	ΔE_p / mV	E_p / mV vs. Fc/Fc^+	I_p / µA	ΔE_p / mV
0.1M TBAP in PC	0.33	11.0	81	-1.36	-5.56	190
$[C_2mim][NTf_2]$	0.31	1.82	95	-1.27	-2.77	393
$[S_{2,2,1}][NTf_2]$	0.30	0.53	83	-1.10	-0.90	n/a
$[C_4mim][NTf_2]$	0.32	1.40	110	-1.10	-1.24	n/a
$[C_6mim][FAP]$	0.42	1.01	93	-1.20	-0.99	278
$[C_4mpyrr][NTf_2]$	0.31	1.31	98	-1.19	-1.02	n/a
$[C_4mim][BF_4]$	0.28	1.97	n/a	-1.11	-1.29	n/a
$[N_{4,1,1,1}][NTf_2]$	0.31	0.60	95	-1.09	-1.00	n/a
$[C_4mim][PF_6]$	0.32	0.54	110	-1.36	-1.34	671
$[P_{14,6,6,6}][NTf_2]$	0.53	2.01	248	n/a	(-1.50)	n/a
$[P_{14,6,6,6}][FAP]$	0.47	0.82	93	n/a	(-0.88)	n/a

The peak-to-peak separations give an indication of the kinetics of the electrochemical step. For the oxidation reaction, a ΔE_p of 81 mV in PC implies a moderately fast electrode process, but not as fast as the ΔE_p of 59 mV expected for an ideal one-electron process.[48] In RTILs, the peak-to-peak separations are similar but slightly larger than PC, ranging from 83–110 mV, suggesting more moderate kinetics in some of the RTILs. The RTIL $[P_{14,6,6,6}][NTf_2]$ displayed a much larger ΔE_p of 248 mV for the oxidation peak, indicating the slowest kinetics out of all the solvents studied. In contrast to the oxidation peaks, the reduction processes are mostly irreversible such that a ΔE_p cannot be measured. Only three RTILs show a reverse peak, and these display much larger peak-to-peak separations compared to the oxidation peak: $[C_2mim][NTf_2]$ (ΔE_p = 393 mV), $[C_6mim][FAP]$ (ΔE_p = 278 mV), and $[C_4mim][PF_6]$ (ΔE_p = 671 mV). They are also wider than the ΔE_p = 190 mV in PC, hence suggesting that the reduction process is highly dependent on the solvation environment.

Redox Behaviour of the Verdazyl Radical at Different Scan Rates

To understand more about the diffusional behaviour of the verdazyl radical in the different solvents, CV was carried out at a range of scan rates from 100 to 2000 mVs^{-1} (Fig. 5). The number of CV scans were minimised due to obvious 'fouling' of the electrode that was observed, particularly at scan rates < 100 mVs^{-1}, likely because of adsorption of electrogenerated products on the electrode. The number of scan rates conducted were limited to four (2000, 1000, 250, 100 mV s^{-1}) in most of the solvents, except for in PC, $[C_2mim][NTf_2]$, $[C_4mim][NTf_2]$, and $[C_4mpyrr][NTf_2]$, where fouling was less noticeable. In these RTILs, fouling could be avoided if the system was left for ~15 mins between scans, presumably due to the slow diffusion of the electrogenerated products away from the surface. Plots of peak current vs scan rate were linear for both oxidation and reduction peaks in all RTILs (see Fig. S4 in the supporting information), suggesting that the electrode processes are diffusion controlled. For voltammetric waves without a clear peak – particularly $[N_{4,1,1,1}][NTf_2]$, $[P_{14,6,6,6}][NTf_2]$, and $[P_{14,6,6,6}][FAP]$ – currents were extracted at fixed potentials where clear peaks exist at lower scan rates.

The peak-to-peak potentials (ΔE_p) for the oxidation peak do not significantly change with scan rate (data not shown), consistent with a relatively fast electrode process. However, in the solvents where reverse peaks are observed, the redox couple for the reduction peak becomes more separated (i.e. increased ΔE_p) with increasing scan rate, consistent with slower kinetics of the reduction process.

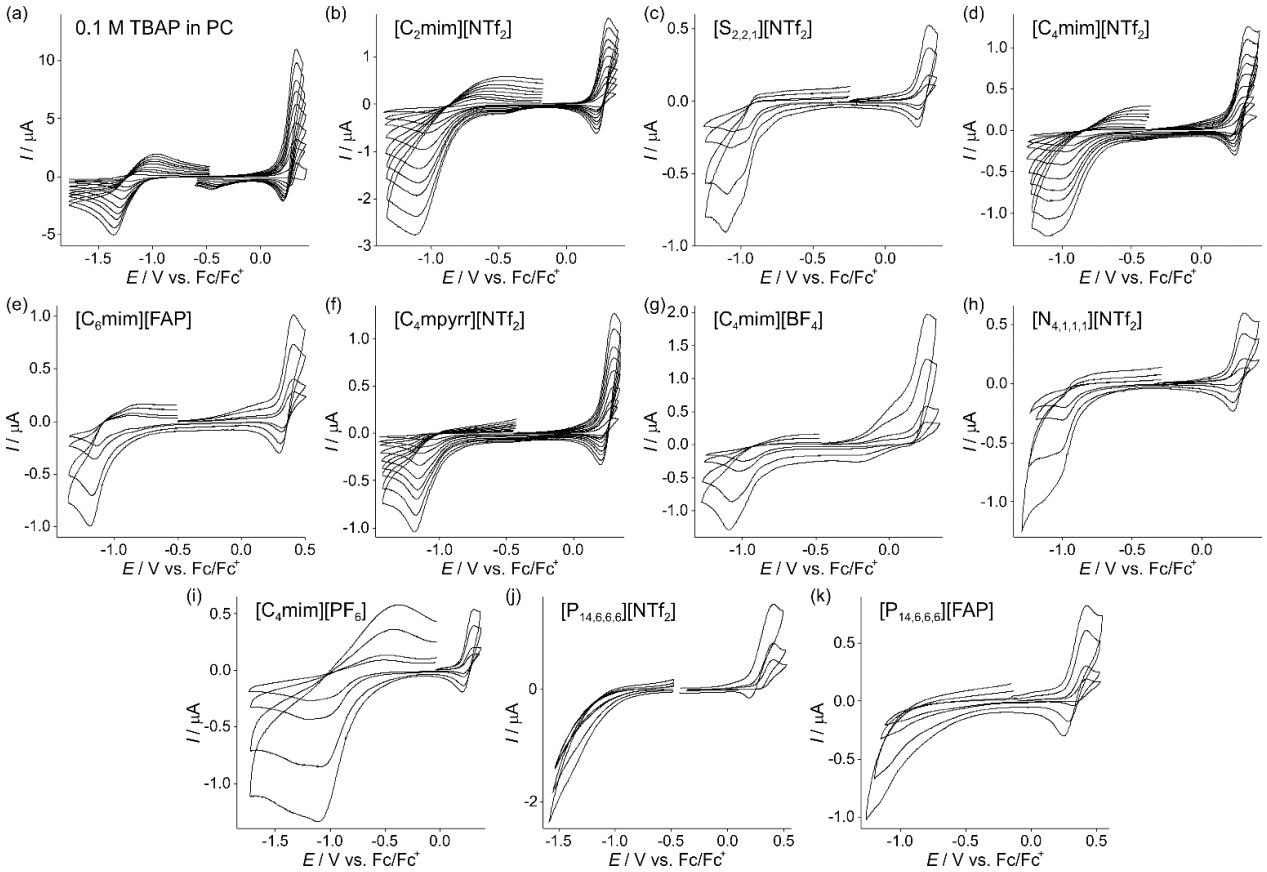

Fig. 5 Cyclic voltammograms at varying scan rates (2000, 1000, 250, 100 mV s^{-1}) of 10 mM MPV on Pt-TFEs in different solvents/RTILs: (a) PC (+0.1 M TBAP), (b) $[C_2mim][NTf_2]$, (c) $[S_{2,2,1}][NTf_2]$, (d) $[C_4mim][NTf_2]$, (e) $[C_6mim][FAP]$, (f) $[C_4mpyrr][NTf_2]$, (g) $[C_4mim][BF_4]$, (h) $[N_{4,1,1,1}][NTf_2]$, (i) $[C_4mim][PF_6]$, (j) $[P_{14,6,6,6}][NTf_2]$ and (k) $[P_{14,6,6,6}][FAP]$ (with selected RTILs carried out at 2000, 1500, 1000, 750, 500, 250, 100, 50, 10 mVs^{-1}). The potentials were shifted with respect to the average potentials of ferrocene/ferrocenium (Fc/Fc^+) peaks.

Due to the good reversibility of the reduction peak in PC, further analysis was undertaken. Fig. 6 shows a plot of the ratio of the reverse current divided by the forward (reduction) peak current. The ratio is highest at slow scan rates and decreases as the scan rate increases. Similar behaviour is also observed for the ratio of the charge under the peaks vs scan rate in PC (see Fig. S5). This behaviour is opposite to what would be expected if a chemical step occurs after the electrochemical step, since faster scan rates would outrun the kinetics of the chemical step such that a larger reverse peak would be observed at high scan rates. Instead, it is possible that differences in the solvation of the neutral radical versus the charged product can lead to different electrode kinetics between the two species due to different solvation/desolvation energies.[49] This is evident in the much more broad nature of the anodic back-peak compared to the reduction peak in PC in Figure 5a. Plots of the reverse/forward peak current ratios for all RTILs are shown in the supporting information (Fig. S6); many of the RTILs follow a similar trend, suggesting a similar behavior is occurring, although this may be combined with follow-up chemical steps in RTILs as discussed above.

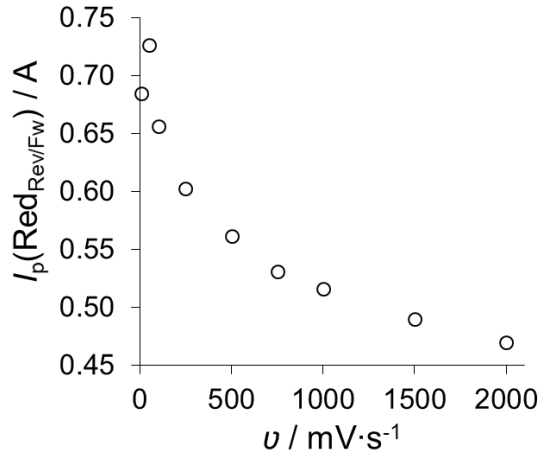

Fig. 6 Plots of the background corrected reverse divided by forward peaks currents of the first reduction peak of 10 mM MPV at different scan rates (Fig. 5) on Pt-TFE in 0.1 M TBAP in PC.

Chronoamperometric analysis

Potential step chronoamperometry was carried out to determine the diffusion coefficient, *D*, of the verdazyl radical in the different solvents. The oxidation peak was chosen for analysis due to the more ideal CV shape compared to the reduction peak, and the oxidative chronoamperometric transient was iteratively fitted to the Shoup and Szabo expression.[40] Table 2 shows the *D* values from the oxidation of the verdazyl radical calculated in PC and the ten different RTILs.

Table 2 Viscosity, η, at 293 K[50-52] of the different solvents, and diffusion coefficients, *D*, for MPV, calculated from fitting chronoamperometric transients to the Shoup and Szabo expression.[40]

RTIL	η / cP	D / m^2 s^{-1} × 10^{-11}
0.1 M TBAP in PC	2.47 [49]	49.7
[C$_2$mim][NTf$_2$]	34 [47]	2.60
[S$_{2,2,1}$][NTf$_2$]	50 [48]	1.30
[C$_4$mim][NTf$_2$]	52 [47]	1.80
[C$_6$mim][FAP]	74 [47]	1.06
[C$_4$mpyrr][NTf$_2$]	89 [47]	1.50
[C$_4$mim][BF$_4$]	112 [47]	0.76
[N$_{4,1,1,1}$][NTf$_2$]	138 [48]	0.76
[C$_4$mim][PF$_6$]	371 [47]	0.31
[P$_{14,6,6,6}$][NTf$_2$]	450 [47]	0.34
[P$_{14,6,6,6}$][FAP]	464 [47]	0.20

According to classic hydrodynamic theory, the diffusion coefficient (*D*) of a species should be inversely proportional to the solvent viscosity (η) in line with the Stokes-Einstein equation: [53]

$$D = \frac{k_B T}{j\pi\eta\alpha} \quad (1)$$

where k_B is the Boltzmann constant, *T* is temperature, α the hydrodynamic radius of the diffusing particle, $j = 4$ is for the 'slip' limit, and $j = 6$ is for the 'stick' limit modes of diffusion. In RTILs, a linear relationship between *D* and the inverse of viscosity is generally observed for neutral compounds such as ferrocene[46], 2,4,6-trinitrotoluene[45], 2,4-dinitrotoluene[54], a rhenium tetrazolato complex (fac-[Re(CO)$_3$(phen)L])[55], the charged cobaltocenium cation[46] and the stable free radical, 2,2,6,6-tetramethylpiperidine-*N*-oxyl (TEMPO)[12]. In most

cases, the 'stick' mode of diffusion is followed in RTILs,[45-46, 55] with some exceptions where *j* is closer to 4, and this behaviour is widely considered to be a "topic of interest".[56-58] For sufficiently small species (e.g. oxygen[44], hydrogen[59], and sulfur dioxide[60]) deviations become more pronounced in RTILs as the molecule is able to move through the small dynamic channels and pores, leading to *D* values that are only partially dependent on the self-diffusion of the solvent itself.[61]

Fig. 7 shows a plot of *D* against the inverse of viscosity, η^{-1}, in the ten RTILs. The diffusion coefficients were 1-2 order of magnitudes smaller in the RTILs than in PC, which is not unexpected, considering the much higher viscosities of the RTILs (Table 2). A reasonably linear fit ($R^2 = 0.907$) was obtained, suggesting that the diffusion of 1,5-dimethyl-3-phenyl-6-oxoverdazyl in RTILs agrees reasonably well with the Stokes-Einstein relationship. From the slope of the fit, the hydrodynamic radius, α, was calculated to be 2.7 Å for the slip limit ($j = 4$), and 4.0 Å for the stick limit ($j = 6$) modes of diffusion. The estimated value of α from the density functional theory (DFT) optimised structure of MPV was 6.5 Å, suggesting that the dominant diffusion mechanism of the radical in RTILs is likely to be the 'stick' mode. However, we note that the presence of additional oxidation processes in the CVs (see supporting information), together with some noticeable fouling of the electrode surface, could affect the reliability of the chronoamperometric fitting, and this should be used as a qualitative guide only.

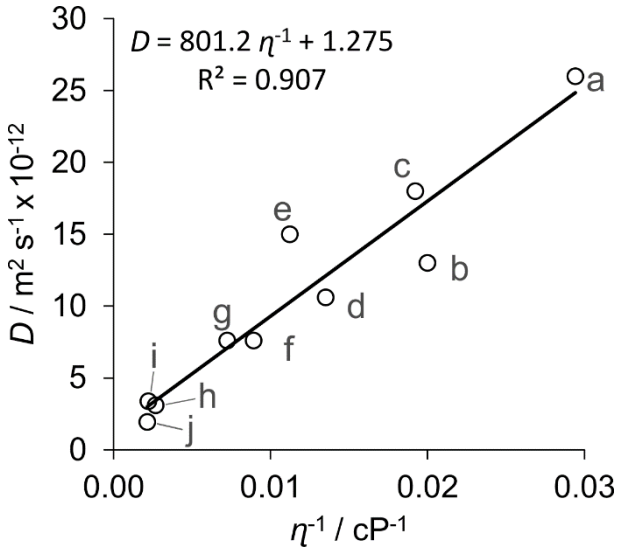

Fig. 7 Plot of the diffusion coefficient vs. 1/viscosity in **(a)** C_2mimNTf$_2$, **(b)** $S_{2,2,1}$NTf$_2$, **(c)** C_4mimNTf$_2$, **(d)** C_6mimFAP, **(e)** C_4mpyrrNTf$_2$, **(f)** C_4mimBF$_4$, **(g)** $N_{4,1,1,1}$NTf$_2$, **(h)** C_4mimPF$_6$, **(i)** $P_{14,6,6,6}$NTf$_2$, and **(j)** $P_{14,6,6,6}$FAP of MPV. The equation and line of best fit, and the associated R^2 of the regression are also shown.

Conclusions

The electrochemical properties of a Type II verdazyl radical – 1,5-dimethyl-3-phenyl-6-oxoverdazyl – has been studied in range of different RTILs and PC. It was found that the solvent environment significantly affected the shapes of the reduction peak, and – to a lesser extent – the oxidation peak. The oxidation peak was chemically reversible in most solvents, but the reduction peak was generally chemically irreversible in the RTILs, also displaying more sluggish kinetics of the electrochemical step. The oxidation peak was analysed by chronoamperometry on a microdisk electrode to extract diffusion coefficients, *D*. The values of *D* for the radical were 1-2 order of magnitudes smaller in the RTILs than in PC, consistent with the viscosity differences. A plot of *D vs*. the inverse of viscosity yielded a reasonably linear fit which suggests that the diffusion of 1,5-dimethyl-3-phenyl-6-oxoverdazyl in RTILs complies with the predictions of simple hydrodynamic theory. Overall, the

results show that different solvent environments significantly influence on the electrochemistry of 1,5-dimethyl-3-phenyl-6-oxoverdazyl, and therefore careful selection of the RTIL is recommended for electrochemical applications using these verdazyl radicals.

Supporting Information

Chemical procedures for the synthesis of 1,5-dimethyl-3-phenyl-6-oxoverdazyl, along with full characterisation of the intermediates. $^{1}H/^{13}C$ NMR and IR spectra of all the intermediates and final product. ESR spectrum of the final radical. Chemical structures of RTIL cations and anions employed in this work. Photo of the verdazyl radical synthesized powder and dissolved in two RTILs. Cyclic voltammetry of the verdazyl radical, showing the wider scan range in PC and the 10 RTILs. Histograms of the peak current and peak potential in the different solvents in order of increasing viscosity. Plots of peak current vs. scan rate in all solvents, plot of charge ratios for the reduction peak as a function of scan rate in PC, and plot of ratio of oxidation to reduction peak current as a function of scan rate in all solvents.

Conflicts of Interest

The authors declare no conflicts of interest.

Acknowledgements

DSS thanks the Australian Research Council (ARC) for funding through a Future Fellowship (FT170100315). ROF thanks the ARC for a Discovery Early Career Research Award (DECRA, DE180100112) and AJM thanks the ARC for the Linkage Infrastructure, Equipment and Facilities grant that was used to purchase the ESR spectrometer at UWA. The authors thank Prof Chris Hardacre (University of Manchester, UK) for the kind donation of one of the RTILs used in this work.

References

[1] D. S. Silvester. Recent advances in the use of ionic liquids for electrochemical sensing. *Analyst*. **2011**, *136*, 4871-4882.

[2] H. Liu, H. Yu. Ionic liquids for electrochemical energy storage devices applications. *J. Mater. Sci. Technol.* **2019**, *35*, 674-686.

[3] I. Osada, H. De Vries, B. Scrosati, S. Passerini. Ionic-Liquid-Based Polymer Electrolytes for Battery Applications. *Angew. Chem. Int. Ed.* **2016**, *55*, 500-513.

[4] M. Armand, F. Endres, D. MacFarlane, H. Ohno, B. Scrosati. ionic-liquid materials for the electrochemical challenges of the future. *Nat. Mater.* **2009**, *8*, 621-629.

[5] M. C. Buzzeo, R. G. Evans, R. G. Compton. Non-Haloaluminate Room-Temperature Ionic Liquids in Electrochemistry–A Review. *Phys. Chem. Chem. Phys.* **2004**, *5*, 1106-1120.

[6] D. R. MacFarlane, N. Tachikawa, M. Forsyth, J. M. Pringle, P. C. Howlett, G. D. Elliott, et al. Energy applications of ionic liquids. *Energ. Environ. Sci.* **2014**, *7*, 232-250.

[7] M. J. Earle, K. R. Seddon. Ionic liquids. Green solvents for the future. *Pure Appl. Chem.* **2000**, *72*, 1391-1398.

[8] F. Endres, S. Zein El Abedin. Air and water stable ionic liquids in physical chemistry. *Phys. Chem. Chem. Phys.* **2006**, *8*, 2101-2116.

[9] P. Wasserscheid, W. Keim. Ionic Liquids- New "Solutions" for Transition Metal Catalysis. *Angew. Chem. Int. Ed.* **2000**, *39*, 3772-3789.

[10] T. Welton. Room-Temperature Ionic Liquids. Solvents for Synthesis and Catalysis. *Chem. Rev.* **1999**, *99*, 2071-2083.

[11] L. E. Barrosse-Antle, A. M. Bond, R. G. Compton, A. M. O 'Mahony, E. I. Rogers, D. S. Silvester. Voltammetry in Room Temperature Ionic Liquids: Comparisons and Contrasts with Conventional Electrochemical Solvents. *Chem. Asian J.* **2010**, *5*, 202-230.

[12] R. G. Evans, A. J. Wain, C. Hardacre, R. G. Compton. An electrochemical and ESR spectroscopic study on the molecular dynamics of TEMPO in room temperature ionic liquid solvents. *ChemPhysChem*. **2005**, *6*, 1035 –1039.

[13] E. I. Rogers, D. S. Silvester, W. E. Ward Jones, L. Aldous, C. Hardacre, A. J. Russell, et al. Electrochemical Kinetics of Ag|Ag+ and TMPD|TMPD+• in the Room-Temperature Ionic Liquid [C4mpyrr][NTf2]; toward Optimizing Reference Electrodes for Voltammetry in RTILs. *J. Phys Chem. C*. **2007**, *111*, 13957-13966.

[14] S. Ernst, K. R. Ward, S. E. Norman, C. Hardacre, R. G. Compton. Changed reactivity of the 1-bromo-4-nitrobenzene radical anion in a room temperature ionic liquid. *Phys. Chem. Chem. Phys.* **2013**, *15*, 6382--6389.

[15] M. M. Islam, T. Imase, T. Okajima, T. M., Y. Niikura, N. Kawashima, et al. Stability of Superoxide Ion in Imidazolium Cation-Based Room-Temperature Ionic Liquids. *J. Phys Chem. A*. **2009**, *113*, 912-916.

[16] R. G. Evans, R. G. Compton. A Kinetic Study of the Reaction between N,N- Dimethyl-p-toluidine and its Electrogenerated Radical Cation in a Room Temperature Ionic Liquid. *ChemPhysChem*. **2006**, *7*, 488-496.

[17] I. D. Brown. Recent Developments in the Methods and Applications of the Bond Valence Model. *Chem. Rev.* **2009**, *109*, 6858-6919.

[18] C. Train, L. Norel, M. Baumgarten. Organic radicals, a promising route towards original molecule-based magnetic materials. *Coord. Chem. Rev.* **2009**, *253*, 2342-2351.

[19] I. Ratera, J. Veciana. Playing with organic radicals as building blocks for functional molecular materials. *Chem. Soc. Rev.* **2012**, *41*, 303-349.

[20] L. Beer, J. L. Brusso, A. W. Cordes, R. C. Haddon, M. E. Itkis, K. Kirschbaum, et al. Resonance-stabilized 1,2,3-dithiazolo-1,2,3-dithiazolyls as neutral π-radical conductors. *J. Am. Chem. Soc.* **2002**, *124*, 9498-9509.

[21] M. Souto, L. Yuan, D. C. Morales, L. Jiang, I. Ratera, C. A. Nijhuis, et al. Tuning the rectification ratio by changing the electronic nature (open-shell and closed-shell) in donor–acceptor self-assembled monolayers. *J. Am. Chem. Soc.* **2017**, *139*, 4262-4265.

[22] K. Nakahara, S. Iwasa, M. Satoh, Y. Morioka, J. Iriyama, M. Suguro, et al. Rechargeable batteries with organic radical cathodes. *Chem. Phys. Lett.* **2002**, *359*, 351-354.

[23] C. Friebe, U. S. Schubert. High-power-density organic radical batteries. *Topics Curr. Chem.* **2017**, *375:19*.

[24] J. B. Gilroy, S. D. J. McKinnon, B. D. Koivisto, R. G. Hicks. Electrochemical studies of verdazyl radicals. *Org. Lett.* **2007**, *9*, 4837-4840.

[25] P. V. Petunin, E. A. Martynko, M. E. Trusova, M. S. Kazantsev, T. V. Rybalova, R. R. Valiev, et al. Verdazyl radical building blocks: synthesis, structure, andsonogashira cross-coupling reactions. *Eur. J. Org. Chem.* **2018**, 4802-4811.

[26] C. Sporer, I. Ratera, D. Ruiz-Molina, Y. Zhao, J. Vidal-Gancedo, K. Wurst, et al. A molecular multiproperty switching array based on the redox behavior of a ferrocenyl polychlorotriphenylmethyl radical. *Angew. Chem. Int. Ed.* **2004**, *43*, 5266-5268.

[27] A. Heckmann, C. Lambert. Neutral organic mixed-valence compounds: Synthesis and all-optical evaluation of electron-transfer parameters. *J. Am. Chem. Soc.* **2007**, *129*, 5515-5527.

[28] R. Kuhn, H. Trischmann. Surprisingly stable nitrogenous free radicals. *Angew. Chem. Int. Ed.* **1963**, *2*, 155-155.

[29] F. A. Neugebauer, H. Fischer. 6-Oxoverdazyls. *Angew. Chem. Int. Ed.* **1980**, *19*, 724-725.

[30] G. N. Lipunova, T. G. Fedorchenko, O. N. Chupakhin. Verdazyls: synthesis, properties, application. *Russ. Chem. Rev.* **2013**, *82*, 701-734.

[31] J. B. Gilroy, S. D. J. McKinnon, P. Kennepohl, M. S. Zsombor, M. J. Ferguson, L. K. Thompson, et al. Probing electronic communication in stable benzene-bridged verdazyl diradicals. *J. Org. Chem.* **2007**, *72*, 8062-8069.

[32] M. J. Plater, J. P. Sinclair, S. Kemp, T. Gelbrich, M. B. Hursthouse, C. J. Gómez-García. New tetrahydro-1,2,4,5-tetrazinan-3-ones and oxoverdazyl free radicals. *J. Chem. Res.* **2006**, 515-520.

[33] R. p. K. a. mechanism. in *Macromol. Symp.* Eds. Buback M, van Herk AM) **2006,** pp. 117-125 (WILEY-VCH Verlag GmbH & Co. KGaA, Welnhelm: Ciocco, Italy).

[34] E. K. Y. Chen, S. J. Teertstra, D. Chan-Seng, P. O. Otieno, R. G. Hicks, M. K. Georges. Verdazyl-mediated living-radical polymerization of styrene and n-butyl acrylate. *Macromolecules*. **2007**, *40*, 8609-8616.

[35] K. Takechi, Y. Kato, Y. Hase. A Highly Concentrated Catholyte Based on a Solvate Ionic Liquid for Rechargeable Flow Batteries. *Adv. Mater.* **2015**, *27*, 2501-2506.

[36] P. A. D. Bonhôte, N. Papageorgiou, K. Kalyanasundaram, M. Grätzel. Hydrophobic, highly conductive ambient-temperature molten salts. *Inorg. Chem.* **1996**, *35*, 1168-1178.

[37] D. R. MacFarlane, P. Meakin, J. Sun, N. Amini. Pyrrolidinium imides: A new family of molten salts and conductive plastic crystal phases. *J. Phys. Chem. B*. **1999**, *103*, 4164-4170.

[38] Y. Wang, J. G. Limon-Petersen, R. G. Compton. Measurement of the diffusion coefficients of $[Ru(NH_3)_6]_3^+$ and $[Ru(NH_3)_6]_2^+$ in

aqueous solution using microelectrode double potential step chronoamperometry. *J. Electro. Chem.* **2010**, *652*, 13–17.
[39] D. S. Silvester, A. J. Wain, L. Aldous, C. Hardacre, R. G. Compton. Electrochemical reduction of nitrobenzene and 4-nitrophenol in the room temperature ionic liquid [C_4dmim][$N(Tf)_2$]. *J. Electroanal. Chem.* **2006**, *596*, 131-140.
[40] D. Shoup, A. Szabo. Chronoamperometric current at finite disk electrodes. *J. Electroanal. Chem.* **1982**, *140*, 237-245.
[41] R. F. Nelson, R. N. Adams. Propylene carbonate: a versatile solvent for electrochemistry and EPR. *J. Electroanal. Chem.* **1967**, *13*, 184-187.
[42] B. A. López de Mishima, H. T. Mishima. Ammonia sensor based on propylene carbonate. *Sensors and Actuators B: Chemical*. **2008**, *131*, 236-240.
[43] S. T. Handy, M. Okello. The 2-Position of Imidazolium Ionic Liquids: Substitution and Exchange. *J. Org. Chem.* **2005**, *70*, 1915-1918.
[44] R. G. Evans, O. V. Klymenko, S. A. Saddoughi, C. Hardacre, R. G. Compton. Electroreduction of oxygen in a series of room temperature ionic liquids composed of group 15-centered cations and anions. *J. Phys. Chem. B*. **2004**, *107*, 7878-7886.
[45] C. Kang, J. Lee, D. S. Silvester. Electroreduction of 2,4,6-trinitrotoluene in room temperature ionic liquids: evidence of an EC_2 mechanism. *J. Phys. Chem. C*. **2016**, *120*, 10997-11005.
[46] E. I. Rogers, D. S. Silvester, D. L. Poole, L. Aldous, C. Hardacre, R. G. Compton. Voltammetric characterization of the ferrocene|ferrocenium and cobaltocenium|cobaltocene redox couples in RTILs. *J. Phys. Chem. C*. **2008**, *112*, 2729-2735.
[47] A. M. O'Mahony, D. S. Silvester, L. Aldous, C. Hardacre, R. G. Compton. Effect of water on the electrochemical window and potential limits of room-temperature ionic liquids. *J. Chem. Eng. Data*. **2008**, *53*, 2884-2891.
[48] A. J. Bard, L. A. Faulkner. *Electrochemical methods: Fundamentals and applications, 2nd edition* **2000** (Wiley-Interscience: New York).
[49] N. Frenzel, J. Hartley, G. Frisch. Voltammetric and spectroscopic study of ferrocene and hexacyanoferrate and the suitability of their redox couples as internal standards in ionic liquids. *Phys. Chem. Chem. Phys.* **2017**, *19*, 28841--28852.
[50] L. E. Barrosse-Antle, A. M. Bond, R. G. Compton, A. M. O'Mahony, E. I. Rogers, D. S. Silvester. Voltammetry in room temperature ionic liquids: Comparisons and contrasts with conventional electrochemical solvents. *Asian J.* **2010**, *5*, 202-230.
[51] A. Bhattacharjee, A. Luís, J. A. Lopes-da-Silva, M. G. Freire, P. J. Carvalho, J. A. P. Coutinhoa. Thermophysical properties of sulfonium- and ammonium-based ionic liquids. *Fluid Ph. Equilibria*. **2014**, *381*, 36-45.
[52] K. M. Prakash, K. H. Dilip. Density and viscosity of propylene carbonate + 2-methoxyethanol at 298.15, 308.15, and 318.15 K. *J. Chem. Eng. Data*. **1995**, *40*, 582-585.
[53] R. G. Compton, C. E. Banks. *Understanding voltammetry, 2nd edition* **2007** (World Scientific: Singapore).
[54] G. Hussain, M. V. Sofianos, J. Lee, C. Gibson, C. E. Buckley, D. Silvester, S. Macroporous platinum electrodes for hydrogen oxidation in ionic liquids. *Electrochem. Commun.* **2018**, *86*, 43–47.
[55] D. S. Silvester, S. U. Uprety, P. J. Wright, M. Massi, S. Stagni, S. M. Muzzioli. Redox properties of a rhenium tetrazolato complex in room temperature ionic liquids: Assessing the applicability of the stokes−einstein equation for a metal complex in ionic liquids. *J. Phys. Chem. C*. **2012**, *116*, 7327−7333.
[56] K. R. J. Lovelock, A. Ejigu, S. F. Loh, S. Men, P. Licence, D. A. Walsh. On the diffusion of ferrocenemethanol in room-temperature ionic liquids: An electrochemical study. *Phys. Chem. Chem. Phys.* **2011**, *13*, 10155– 10164.
[57] A. W. Taylor, P. Licence, A. P. Abbott. Non-classical diffusion in ionic liquids. *Phys. Chem. Chem. Phys.* **2011**, *13*, 10147– 10154.
[58] M. A. Vorotyntsev, V. A. Zinovyeva, M. Picquet. Diffusional transport in ionic liquids: Stokes–Einstein relation or "sliding sphere" model? Ferrocene (FC) in imidazolium liquids. *Electrochim. Acta*. **2010**, *55*, 5063– 5070.
[59] D. S. Silvester, K. L. Ward, L. Aldous, C. Hardacre. The electrochemical oxidation of hydrogen at activated platinum electrodes in room temperature ionic liquids as solvents. *J. Electroanal. Chem.* **2008**, *618*, 53-60.
[60] L. E. Barrosse-Antle, D. S. Silvester, L. Aldous, C. Hardacre, R. G. Compton. Electroreduction of sulfur dioxide in some room-temperature ionic liquids. *J. Phys. Chem. C*. **2008**, *112*, 3398-3404.
[61] J. C. Araque, S. K. Yadav, M. Shadeck, M. Maroncelli, C. J. Margulis. How is diffusion of neutral and charged tracers related to the structure and dynamics of a room-temperature ionic liquid? Large deviations from stokes–einstein behavior explained. *J. Phys. Chem. B.* **2015**, *119*, 7015-7029.